

Supplementary Figure 1

A, Correlation between LHX1 expression and DFI in HNSCC patients. **B**, Correlation between LHX1 expression and DSS in HNSCC patients. **C**, Correlation between LHX1 expression and tumor size in HNSCC patients. **D**, Correlation between LHX1 expression and lymph node metastasis in HNSCC. **E**, Correlation between LHX1 expression and distant metastasis in HNSCC patients. **F**, Correlation between LHX1 expression and clinical stage in HNSCC. **G**, Correlation of LHX1 expression with pathological grade in HNSCC. **H**, Correlation between LHX1 expression and age in HNSCC patients. **I**, Correlation between LHX1 expression and gender in HNSCC patients. *, $P < 0.05$; **, $P < 0.01$; ***, $P < 0.001$; ****, $P < 0.0001$; ns, not significant.

Supplementary Figure 2

A, GSEA was performed following *LHX1* knockout, revealing the downregulated pathways. **B**, Immunoblotting of LHX1 following the LHX1 overexpression. **C**, RT-qPCR analysis of *LHX1* following LHX1 overexpression. $n = 3$, unpaired *t* test. **D**, RT-qPCR analysis of *ALDH1A1*, *SOX2*, *POU5F1*, and *NANOG* following LHX1 overexpression. **E**, TIF of tumor cells assessed by the ELDA method following LHX1 overexpression. $n = 8$, χ^2 test. Data are shown as mean \pm SD. **, $P < 0.01$; ***, $P < 0.001$; ****, $P < 0.0001$.

Supplementary Figure 3

A, The protein levels of IL-1 α , IL-6, and IL-8 measured by ELISA in *LHX1*-knockout cells following treatment with SASP inhibitors. **B**, RT-qPCR analysis of *IL1A*, *IL6*, *IL8*,

and *CXCL10* following LHX1 overexpression. $n = 3$, unpaired *t* test. **C**, Immunoblotting of pRb, p21, and p16 following LHX1 overexpression. **D**, Colony formation assay in *LHX1*-knockout cells following treatment with SASP inhibitors. **E**, Quantification of the colony numbers in *LHX1*-knockout cells following treatment with SASP inhibitors. $n = 3$, one-way ANOVA. **F**, RT-qPCR analysis of *SOX2*, *POU5F1*, and *NANOG* in *LHX1*-knockout cells following treatment with SASP inhibitors. $n = 3$, one-way ANOVA. Data are shown as mean \pm SD. *, $P < 0.05$; **, $P < 0.01$; ***, $P < 0.001$; ns, not significant.

Supplementary Figure 4

A, Colony formation assay in recipient cells following treatment with CM from *LHX1*-knockout cells. **B**, Quantification of the colony numbers. $n = 3$, unpaired *t* test. **C**, Sphere formation assay in recipient cells following treatment with conditioned medium from *LHX1*-knockout cells. Scale bar, 100 μ m. **D**, Quantification of the sphere numbers in recipient cells. $n = 3$, unpaired *t* test. **E**, RT-qPCR analysis of *ALDHA1*, *SOX2*, *POU5F1*, and *NANOG* in recipient cells following treatment with CM from *LHX1*-knockout cells. $n = 3$, unpaired *t* test. **F**, Immunoblotting of pRb, p21, and p16 in *LHX1*-knockout cells following treatment with neutralizing-antibodies. **G**, Colony formation assay in *LHX1*-knockout cells following treatment with neutralizing-antibodies. **H**, Sphere formation assay in *LHX1*-knockout cells following treatment with neutralizing-antibodies. Scale bar, 100 μ m. **I**, Quantification of the colony numbers. $n = 3$, one-way ANOVA. **J**, Quantification of the sphere numbers. $n = 3$, one-way ANOVA. Data are shown as mean \pm SD. *, $P < 0.05$; **, $P < 0.01$; ***, $P < 0.001$; ****, $P < 0.0001$; ns,

not significant.

Supplementary Figure 5

A, The counts value of *cGAS* and *STING* following *LHX1* knockout. **B**, RT-qPCR analysis of *STING* in *LHX1* knockout FaDu cells. $n = 3$, one-way ANOVA. **C**, Immunoblotting analysis of STING, P-TBK1, TBK1, P-IRF3, and IRF3 in *LHX1* knockout FaDu cells. **D**, RT-qPCR analysis of *STING* following *LHX1* overexpression. $n = 3$, unpaired *t* test. **E**, Immunoblotting analysis of STING following *LHX1* overexpression. **F**, RT-qPCR analysis of *cGAS* following *LHX1* knockout. $n = 3$, one-way ANOVA. **G**, RT-qPCR analysis of *cGAS* following *LHX1* overexpression. $n = 3$, unpaired *t* test. **H**, ELISA analysis of cGAMP in normal epithelial cells (HIOEC and HaCaT) and HNSCC cells (CAL27 and FaDu). **I**, ELISA analysis of cGAMP following *LHX1* knockout. **J**, ELISA analysis of cGAMP following *LHX1* overexpression. **K**, Immunoblotting analysis of STING following re-expression of *LHX1*-WT, *LHX1*-ΔLIM, and *LHX1*-ΔHOX in *LHX1* knockout FaDu cells. **L**, RT-qPCR analysis of *STING* following re-expression of *LHX1*-WT, *LHX1*-ΔLIM, and *LHX1*-ΔHOX in *LHX1* knockout FaDu cells. $n = 3$, one-way ANOVA. **M**, ChIP-PCR analysis of *LHX1* binding to different regions of the *STING* promoter in FaDu cells. **N**, ChIP-qPCR analysis of *LHX1* binding to different regions of the *STING* promoter in FaDu cells. $n = 3$, unpaired *t* test. Data are shown as mean \pm SD. *, $P < 0.05$; **, $P < 0.01$; ***, $P < 0.001$; ****, $P < 0.0001$; ns, not significant.

Supplementary Figure 6

A, Expression of *STING* in HNSCC and normal tissues from the TCGA database. $n = 518$ for tumors, $n = 44$ for normal tissues, unpaired t test. **B**, Promoter methylation level of *STING* in HNSCC and normal tissues from the TCGA database. $n = 50$ for normal tissues, $n = 528$ for tumors, unpaired t test. **C**, ChIP-qPCR analysis of H3K9me3 and H3K27me3 at the *STING* promoter following *LHX1*-knockout. $n = 3$, unpaired t test. **D**, Immunoblotting of pRb, p21, and p16 in *LHX1*-knockout cells following treatment with cGAMP. **E**, Colony formation assay in *LHX1*-knockout cells following treatment with cGAMP. **F**, Quantification of the colony numbers. $n = 3$, one-way ANOVA. Data are shown as mean \pm SD. ***, $P < 0.001$; ns, not significant.

Supplementary Figure 7

A, The amino acid sequences of the LIM1 and LIM2 domains, as well as the sequences of the designed TAT, TAT-AE, and TAT-VM peptides. **B**, RT-qPCR analysis of *STING* in FaDu cells following treatment with different concentrations of TAT. **C**, RT-qPCR analysis of *STING* expression in FaDu cells when treated with different concentrations of TAT-AE and TAT-VM peptides. **D**, Co-IP results of HA-LDB1 and FLAG-LHX1 in 293T cells when treated with TAT-AE and TAT-VM peptides. **E**, RT-qPCR analysis of *STING* in HNSCC cells when treated with TAT-AE or TAT-VM peptides. $n = 3$, unpaired t test. **F**, Immunoblotting analysis of STING in HNSCC cells treated with TAT-AE and TAT-VM peptides. **G**, Colony formation assay following treatment with TAT-AE-DRI and TAT-VM-DRI peptides. **H**, Quantification of the colony numbers. $n = 3$,

one-way ANOVA. **I**, Effect of TAT-AE-DRI and TAT-VM-DRI peptides on the growth of CAL27-derived subcutaneous xenografts. $n = 8$, unpaired t test. **J**, Impact of TAT-AE-DRI and TAT-VM-DRI peptides on the survival of mice in the MOC2 orthotopic tongue tumor model. $n = 8$, Kaplan-Meier curve. Data are shown as mean \pm SD. *** $P < 0.001$; **** $P < 0.0001$.

Supplementary Figure 8

A, Immunoblotting analysis of STING following LDB1 overexpression. **B**, RT-qPCR analysis of *STING* following LDB1 overexpression. $n = 3$, unpaired t test. **C**, Immunoblotting analysis of STING following *LDB1*-knockout. **D**, RT-qPCR analysis of *STING* following *LDB1*-knockout. $n = 3$, one-way ANOVA. **E**, Co-IP results of FLAG-LHX1 and HA-LDB1 in 293T cells, with FLAG-LHX1 serving as the bait protein. **F**, Co-IP results of HA-LDB1 and FLAG-LHX1 in 293T cells, with HA-LDB1 serving as the bait protein. **G**, Sequence diagram of the LDB1-WT and LDB1-ΔLID mutant. **H**, RT-qPCR analysis of *STING* following re-expression of LDB1-WT and LDB1-ΔLID mutant in *LDB1*-knockout FaDu cells. $n = 3$, one-way ANOVA. **I**, Immunoblotting analysis of STING following re-expression of LDB1-WT and LDB1-ΔLID mutant in *LDB1*-knockout FaDu cells. **J**, ChIP-PCR analysis of the binding of LHX1-WT and LHX1-3m mutant to the site1 region of *STING* promoter in FaDu cells. **K**, ChIP-qPCR analysis of the binding of LHX1-WT and LHX1-3m mutant to the site1 region of *STING* promoter in FaDu cells. $n = 3$, one-way ANOVA. **L**, RT-qPCR analysis of *STING* following re-expression of LHX1-WT or LHX1-3m mutant in *LHX1*

knockout FaDu cells. $n = 3$, one-way ANOVA. **M**, Immunoblotting analysis of STING following re-expression of LHX1-WT or LHX1-3m mutant in *LHX1* knockout FaDu cells. Data are shown as mean \pm SD. **, $P < 0.01$; ***, $P < 0.001$; ****, $P < 0.0001$; ns, not significant.

Supplementary Figure 9

A, The amino acid sequences of the LIM1 and LIM2 domains, as well as the sequences of the designed TAT, TAT-AE, and TAT-VM peptides. **B**, Fluorescence microscopy images of FaDu with peptides conjugated to GFP protein. Scale bar, 50 μ m. **C**, RT-qPCR analysis of *STING* in FaDu cells following treatment with different concentrations of TAT. **D**, RT-qPCR analysis of *STING* expression in FaDu cells when treated with different concentrations of TAT-AE and TAT-VM peptides. **E**, Co-IP results of HA-LDB1 and FLAG-LHX1 in 293T cells when treated with TAT-AE and TAT-VM peptides. **F**, RT-qPCR analysis of *STING* in HNSCC cells when treated with TAT-AE or TAT-VM peptides. $n = 3$, unpaired *t* test. **G**, Immunoblotting analysis of STING in HNSCC cells treated with TAT-AE and TAT-VM peptides. **H**, Co-IP results of LDB1 and LHX1, LMO1, LMO2 in FaDu cells when treated with TAT-AE-DRI and TAT-VM-DRI peptides. **I**, Colony formation assay following treatment with TAT-AE-DRI and TAT-VM-DRI peptides. **J**, Quantification of the colony numbers. $n = 3$, one-way ANOVA. $n = 8$, Kaplan-Meier curve. Data are shown as mean \pm SD. ***, $P < 0.001$; ****, $P < 0.0001$.

Supplementary Figure 10

A, Effect of TAT-AE-DRI and TAT-VM-DRI peptides on the growth of CAL27-derived subcutaneous xenografts. $n = 8$, unpaired t test. **B**, Impact of TAT-AE-DRI and TAT-VM-DRI peptides on the survival of mice in the MOC2 orthotopic tongue tumor model. $n = 8$, Kaplan-Meier curve. **C**, IHC staining of Ki67, Cleaved Caspase-3, STING, p-TBK1, and p-IRF3 in tumor tissues from mice in the MOC1 orthotopic tongue tumor model. Scale bar, 50 μ m. **D**, Statistical analysis of relative repression of Ki67, Cleaved Caspase-3, STING, p-TBK1, and p-IRF3. $n = 8$, unpaired t test. Data are shown as mean \pm SD. **** $P < 0.0001$; ns, not significant.

Figure S1

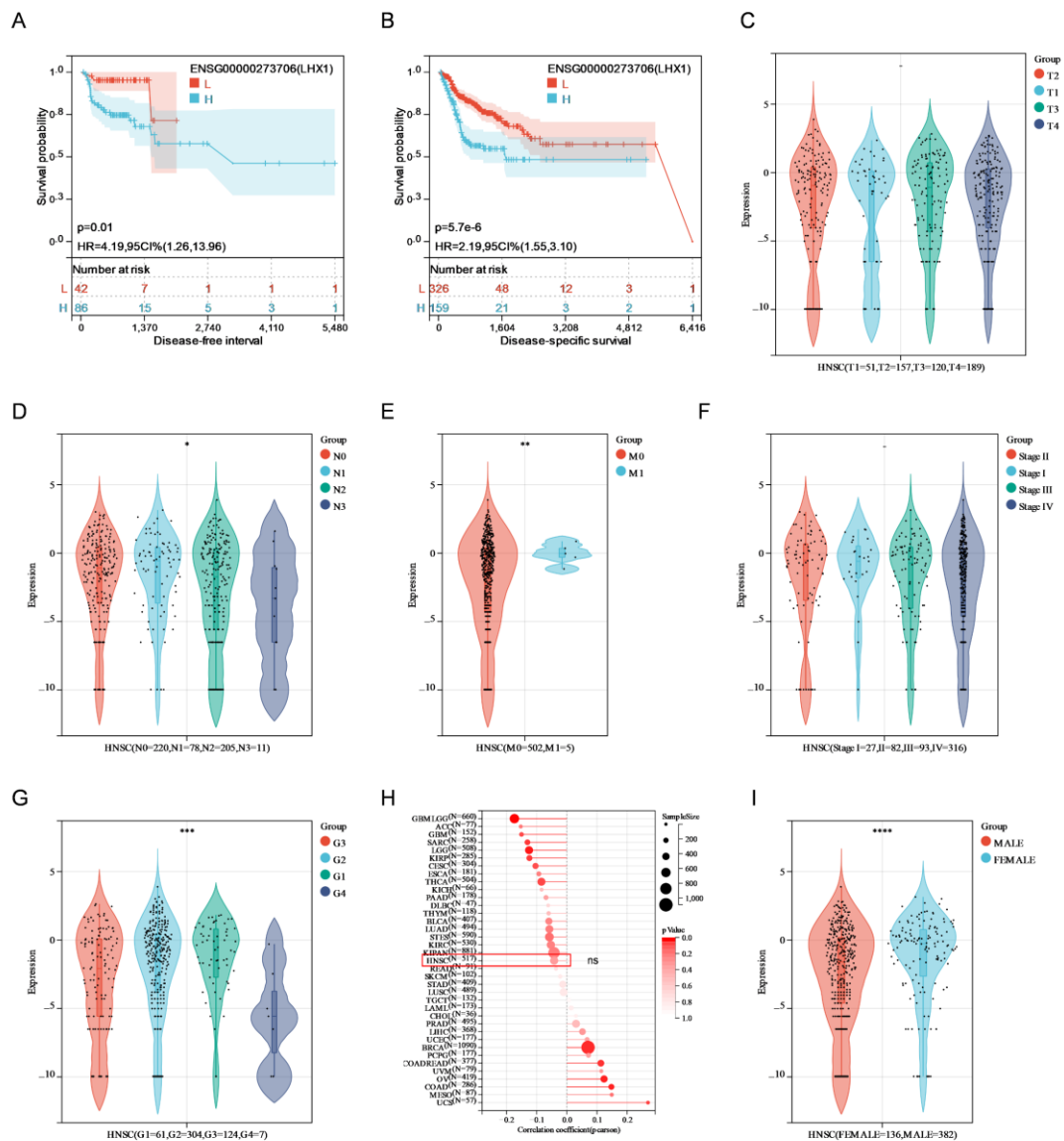


Figure S2

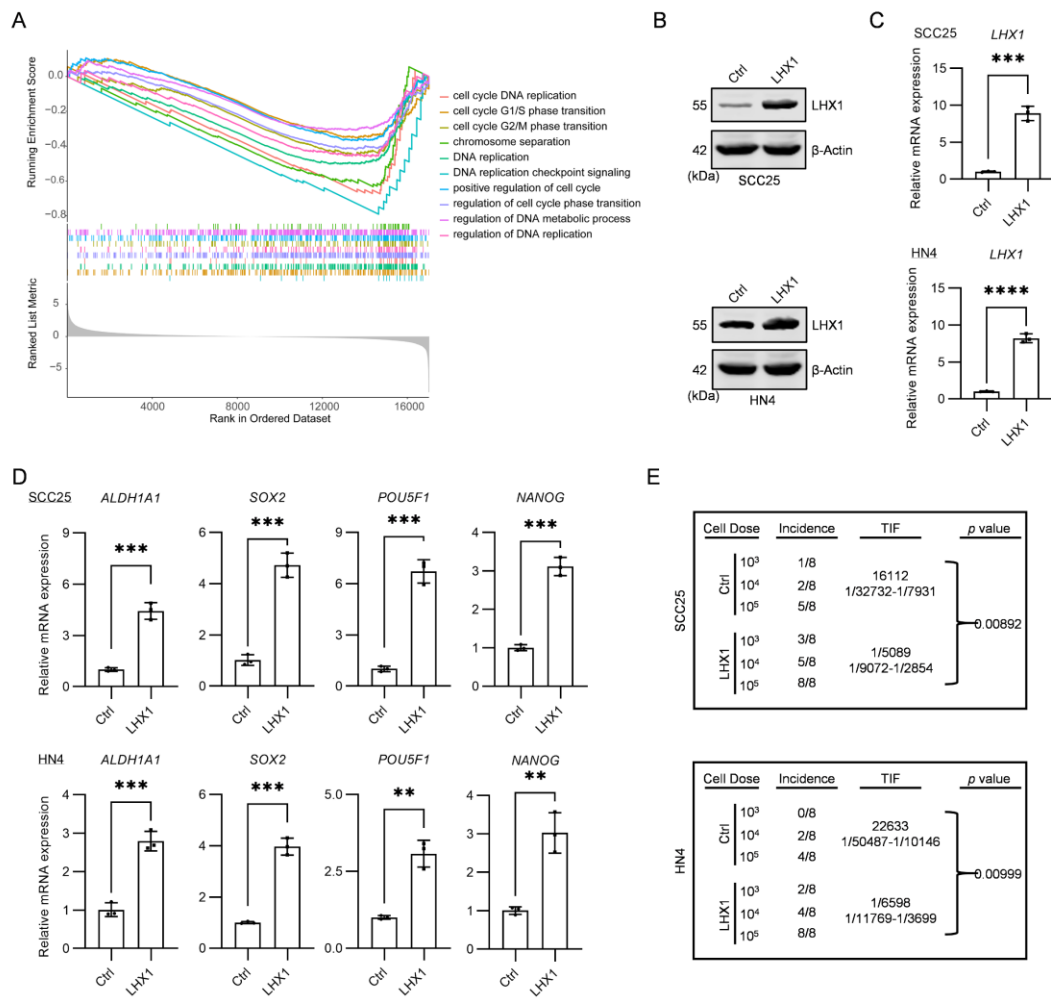
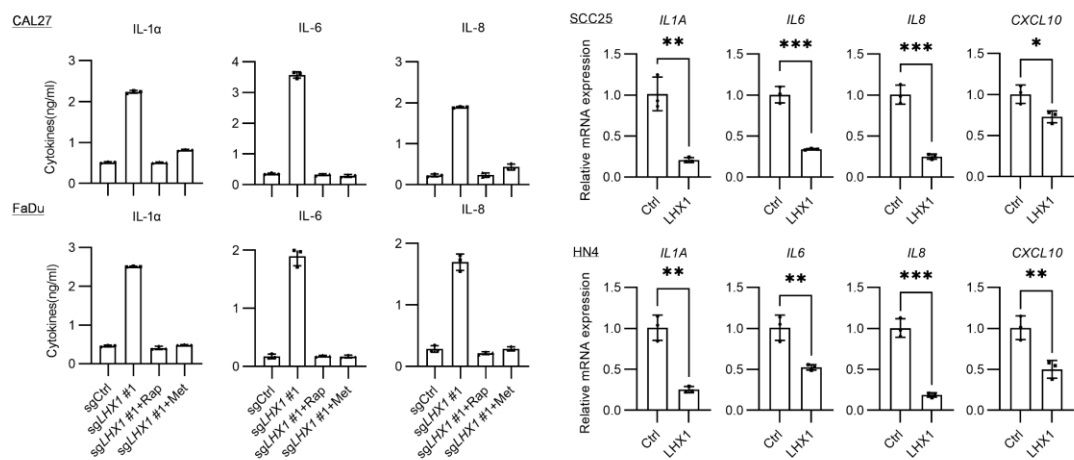
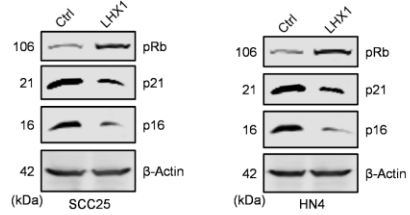


Figure S3

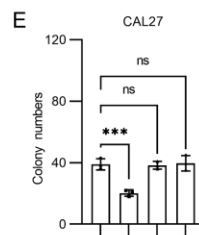
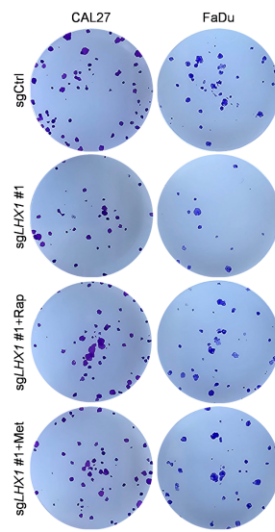
A



C



D



F

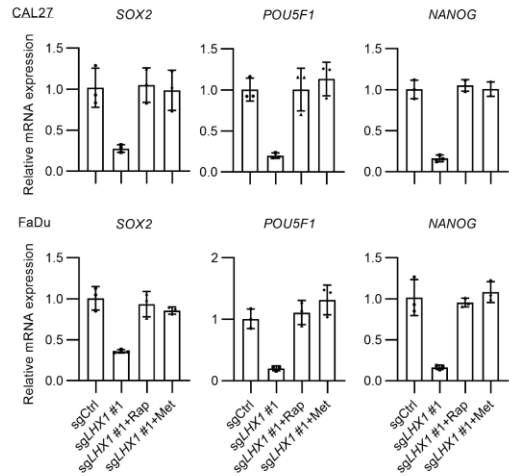


Figure S4

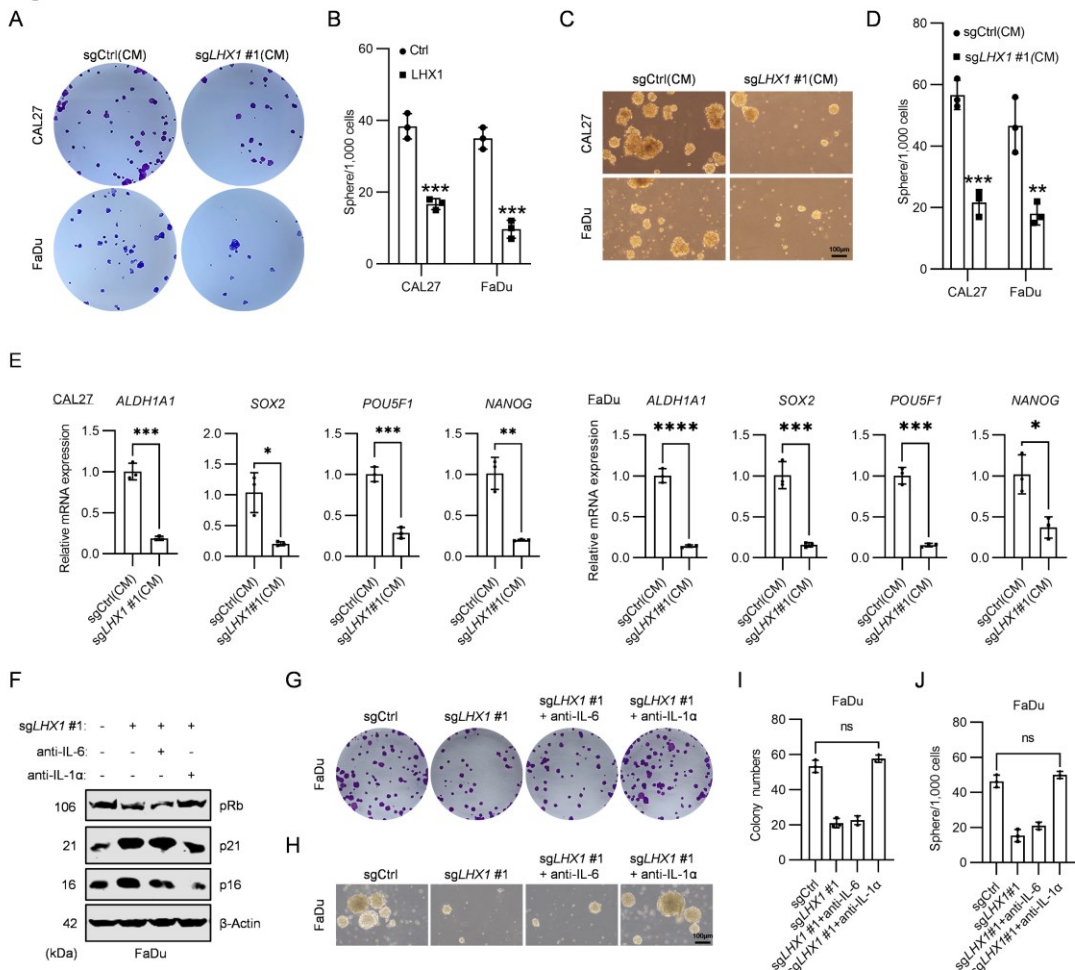


Figure S5

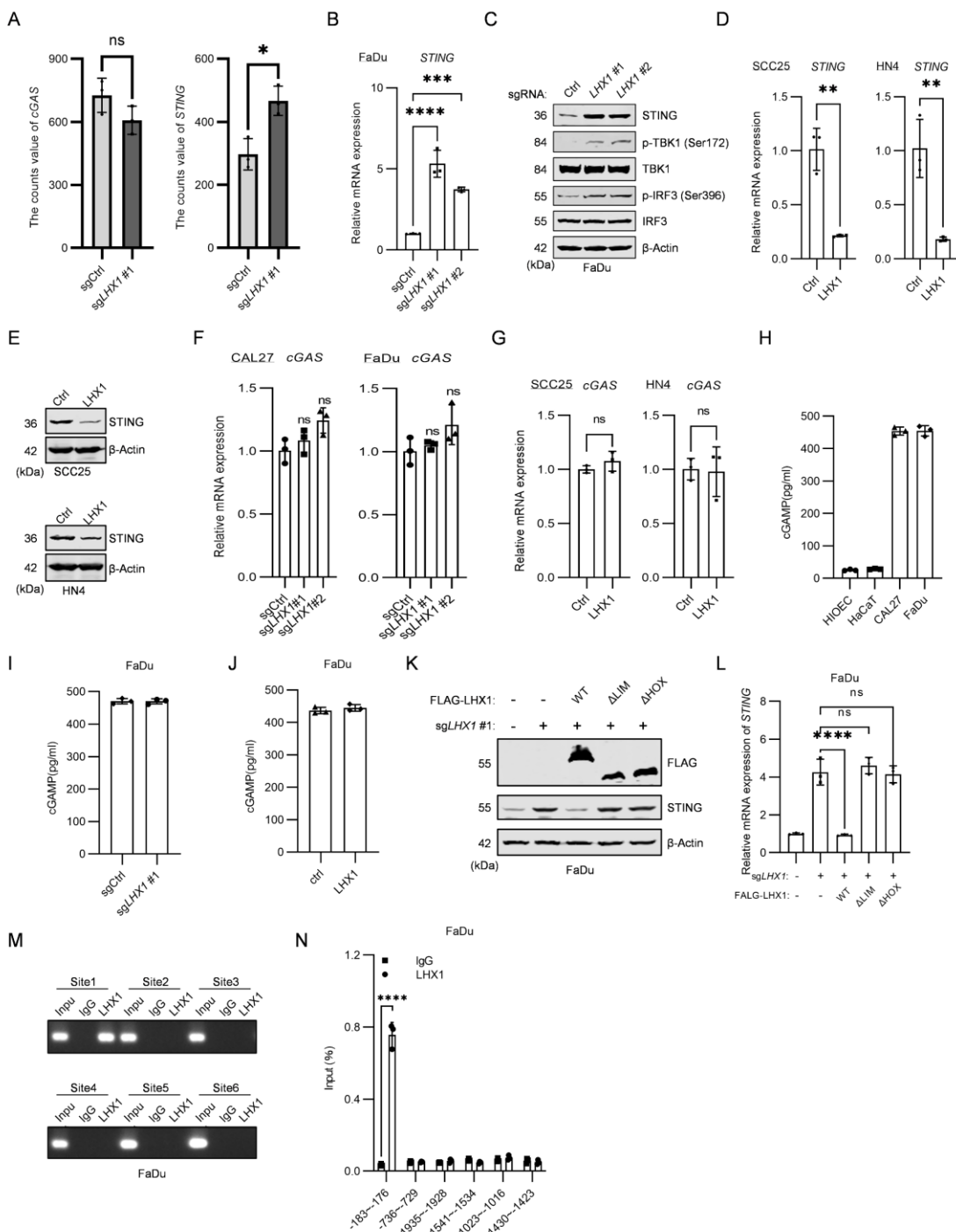


Figure S6

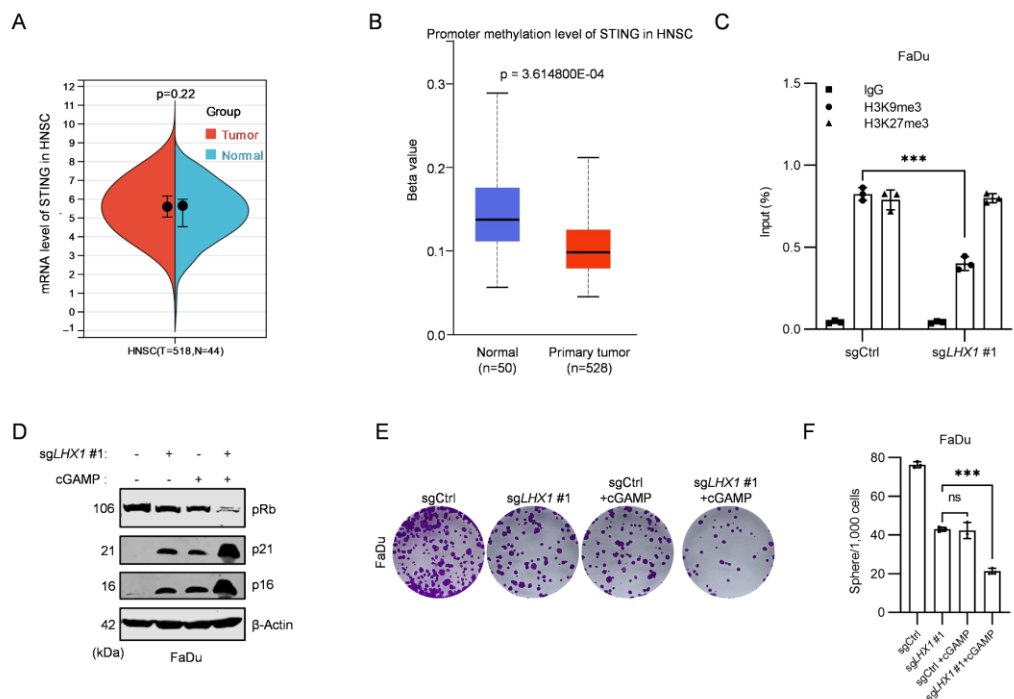


Figure S7

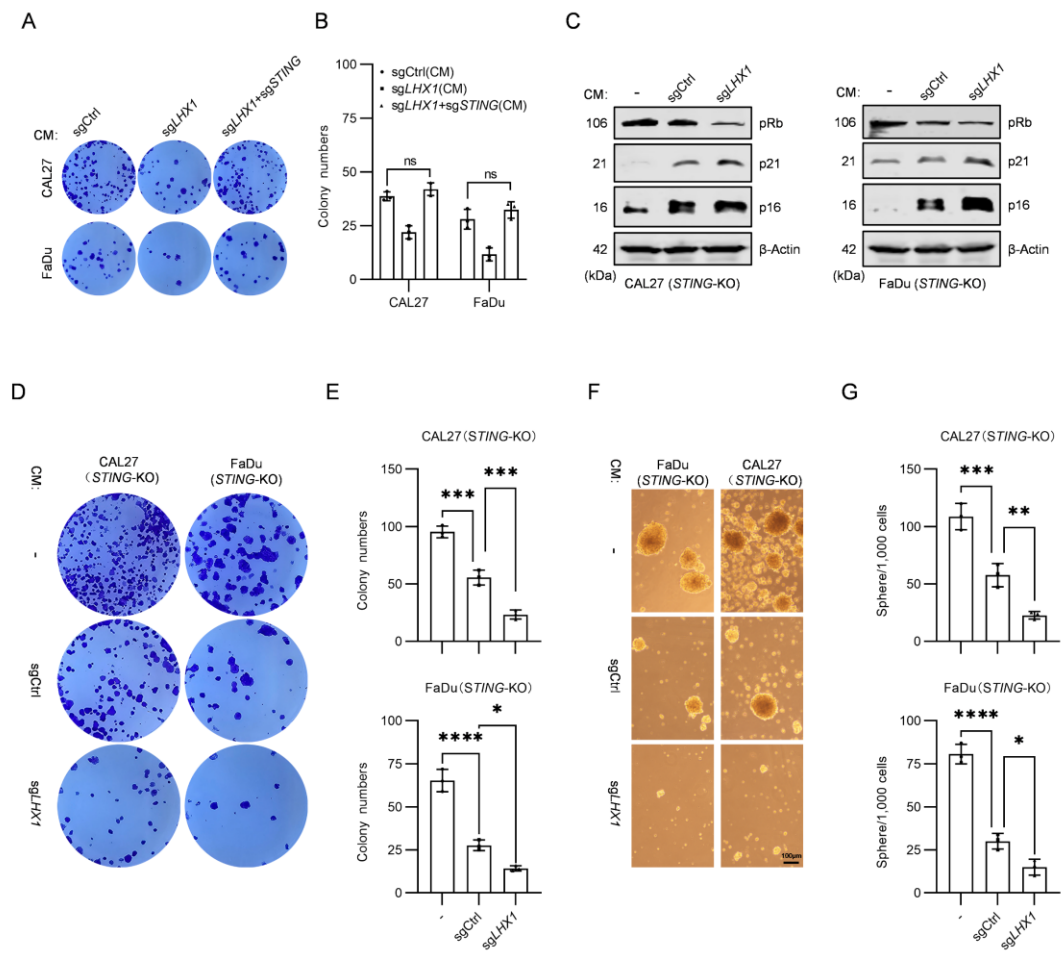


Figure S8

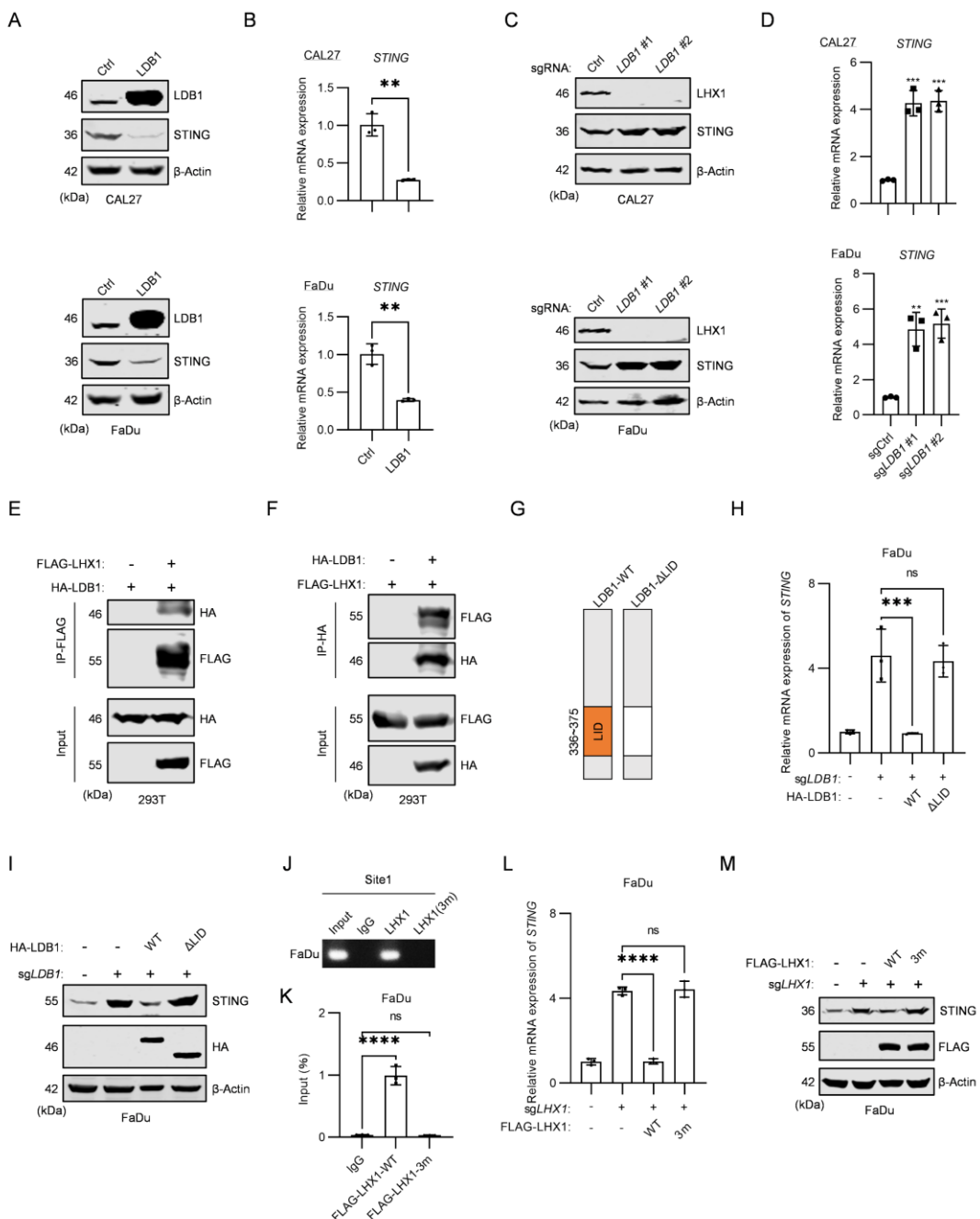


Figure S9

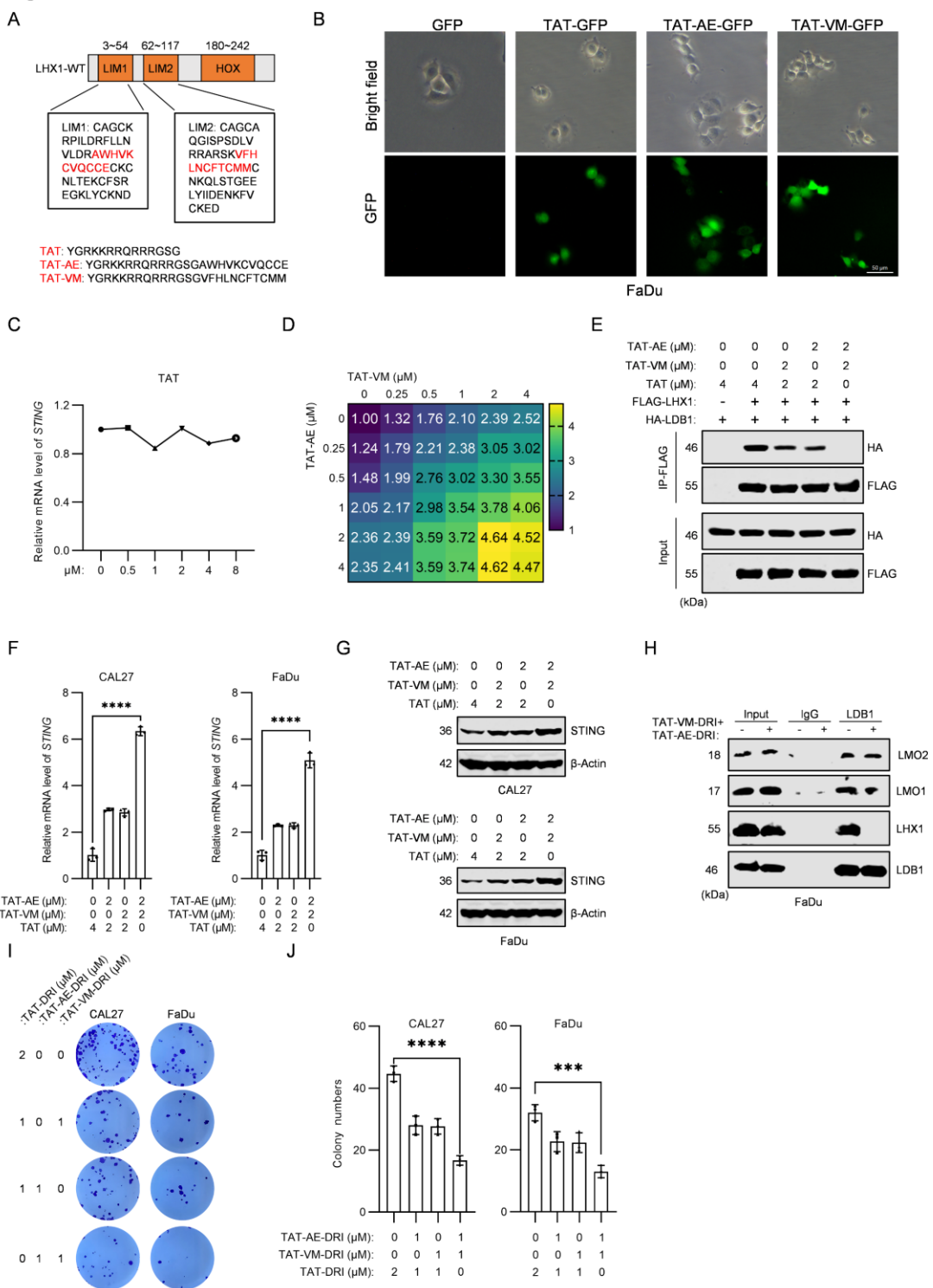


Figure S10

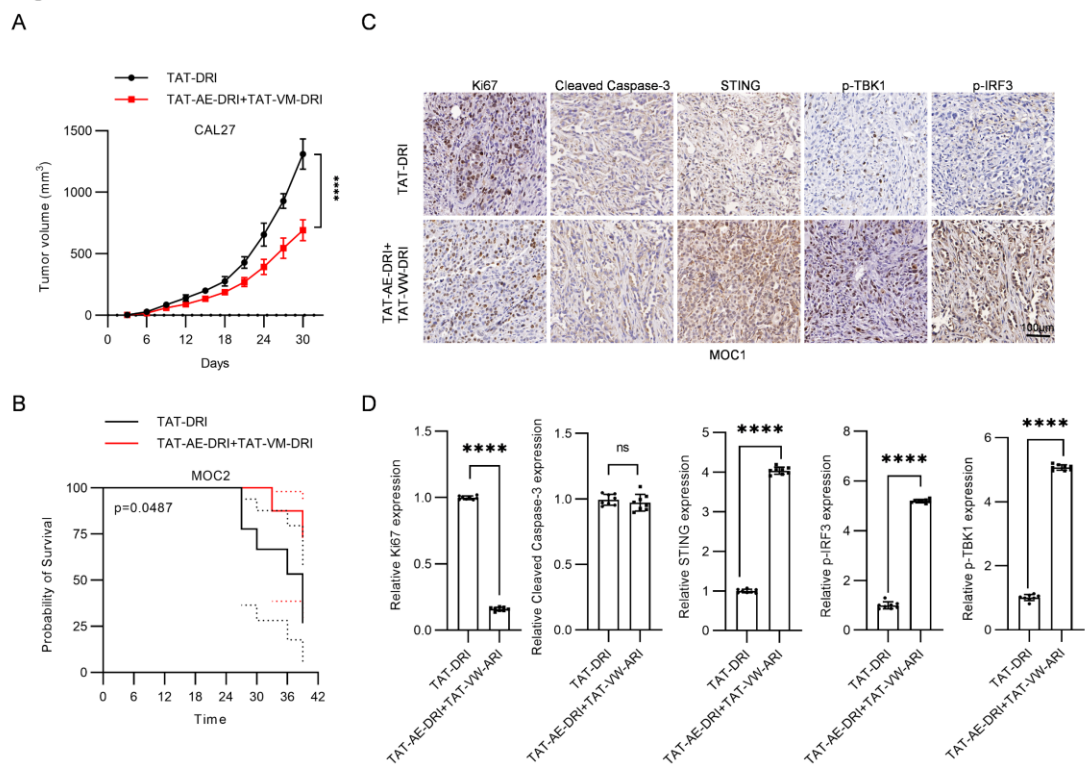


Table S1. Detailed information of patients.

Patients	Age	Location	TNM	Relapse	Grade
1	53	Mouth Floor	T3N0M0	NO	II-III
2	55	Buccal Mucosa	T2N1M0	NO	II
3	67	Buccal Mucosa	T2N0M0	NO	I-II
4	46	Tongue	T2N1M0	YES	III
5	39	Tongue	T3N1M0	NO	III
6	72	Gingiva	T2N0M0	NO	II
7	73	Buccal Mucosa	T1N0M0	NO	I-II
8	71	Gingiva	T2N0M0	YES	II-III
9	71	Tongue	T3N0M0	YES	III
10	48	Tongue	T1N0M0	NO	I-II
11	62	Buccal Mucosa	T2N0M0	NO	II
12	57	Buccal Mucosa	T2N0M0	NO	II
13	37	Tongue	T3N1M0	NO	III
14	32	Tongue	T3N0M0	YES	II-III
15	75	Tongue	T2N0M0	NO	II
16	34	Tongue	T2N0M0	NO	II
17	48	Tongue	T1N0M0	NO	I
18	69	Soft Palate	T2N1M0	NO	III
19	49	Tongue	T1N2M0	NO	IV
20	44	Buccal Mucosa	T3N1M0	NO	III
21	36	Tongue	T3N0M0	YES	II-III

Table S2. The primers for sgRNAs.

Genes	Species	Primers
Ctrl	Human	F: CACCGACGGAGGCTAACCGTCGCAA R: AAACCTTGCACGCTTAGCCTCCGTC
<i>LHX1</i> #1	Human	F: CACCGTCTCCGCACCAGGTCGCTAG R: AAACCTAGCGACCTGGTGCAGGAGAC
<i>LHX1</i> #2	Human	F: CACCGCGGCTGCAAAAGGCCATCC R: AAACGGATGGGCCTTTGCAGCCGC
<i>STING</i>	Human	F: CACCGCTGGACTGCTGTTAACCG R: AAACCGTTAACAGCAGTCCCAGC
<i>LDB1</i> #1	Human	F: CACCGGAAAGGCCTGCCGTTGG R: AAACCCGAACGGCAACGCCCTTCC
<i>LDB1</i> #2	Human	F: CACCGGAGTGTGACAATCTCTGGT R: AAACACCAGAGATTGTACACTCC

Table S3. The primers used for RT-qPCR.

Genes	Species	Primers
<i>ACTB</i>	Human	F: CCTGGCACCCAGCACAAT R: GGGCCGGACTCGTCATAC
<i>LHX1</i>	Human	F: GCCCACCCGCCACATCC R: TGCTTCATCCTCCGCTCCTTG
<i>ALDHIA1</i>	Human	F: CCGTGGCGTACTATGGATGC R: GCAGCAGACGATCTCTTCGAT
<i>SOX2</i>	Human	F: GCCGAGTGGAAACTTTGTCG R: GGCAGCGTGTACTTATCCTTCT
<i>POU5F1</i>	Human	F: CTGGGTTGATCCTCGGACCT R: CCATCGGAGTTGCTCTCCA
<i>NANOG</i>	Human	F: CCCCAGCCTTACTCTTCCTA R: CCAGGTTGAATTGTTCCAGGTC
<i>IL1A</i>	Human	F: TGGTAGTAGCAACCAACGGGA R: ACTTGATTGAGGGCGTCATT
<i>IL6</i>	Human	F: ACTCACCTCTTCAGAACGAATTG R: CCATCTTGAAGGTTCAGGTTG
<i>IL8</i>	Human	F: TTTTGCCAAGGAGTGCTAAAGA R: AACCCCTCTGCACCCAGTTTC
<i>CXCL10</i>	Human	F: CACCATGAATCAAAC TGC R: GCTGATGCAGGTACAGCGT
<i>STING1</i>	Human	F: CTAGGAGAGCCACCAGAGCAC R: AGAAATAGATGGACAGCAGAACAG
<i>cGAS</i>	Human	F: AAGAAGAACATGGCGGCTATCC R: AAGGCTGAGGCAGGAGAATGG

Table S4. The primers used in the ChIP assay.

Binding sites	Binding sequence	Primers
Site1	GCAATTAC	F: CGGCCTCCAAAGCGCTGGG R: GGTTTCTGCCAGAAGGCAG
Site2	TCAATTAC	F: CAGAGCAAGCTGGGCTTGG R: TTTTATAGATGGATAATCCG
Site3	CCAATTAT	F: GTCTATTTCACGTTAGGT R: GGCTGGGTTCCCCACTCAT
Site4	GCCATCAC	F: AAGCAGTTCTCCTGCCTCAG R: CAACATGGAGAAACCCCATC
Site5	GCCATCAC	F: TTTTTTGAGATAGGGTATC R: CTGAGGTGGGAGCATCACTT
Site6	GCAATTG	F: AGGATGGTCTTGAACCTCTG R: CGGCAACAAAGAGTCAAAC